Design and evaluation of a thermal actuator for ultra-precision machining

L. Schönemann*, P. Mejia, O. Riemer, E. Brinksmeier
LFM Laboratory for Precision Machining, Universität Bremen, Badgasteiner Straße 2, 28359 Bremen, Germany
**schoenemann@lfm.uni-bremen.de*

Abstract

Diamond milling of optical and freeform surfaces is usually considered to be a particularly slow machining process, as only one diamond tool with one cutting edge can be applied (i.e. fly-cutting). The reason lies in the tight tolerances of the machined surface, which are in the nanometre range.

A novel attempt to enable an ultra-precise adjustment of multiple diamond tools is the use of controlled thermal expansion as actuating mechanism. The idea is to locally heat up the tool holder via a high-performance light source (i.e. IR-LED or laser) in order to induce a thermal elongation of the substrate material.

This paper will present the initial design of such a thermal actuator on the basis of thermal and mechanical simulations. Furthermore, a first evaluation of such an actuator in a static test stand will be given.

1 Ultra-precision milling with multiple diamond tools

Ultra-precision machining with single crystal diamond tools is considered to be one of the most versatile processes for machining optical surfaces and microstructures [1-3]. Apart from its limited spectrum of machinable workpiece materials [4], the main disadvantage of this technology is its time-consuming machining speed [5]. Under normal conditions, spindles are used up to 1500 or 2000 rpm and the applied feedrate and cutting velocity are in the range of a few hundred millimetres per minute. Consequently, even the machining of small optical surfaces can take several hours up to days of machining time.

A simple measure to increase the productivity of ultra-precision milling operations would be to use multiple cutting edges in one setup, as it is common in conventional machining. However, due to the tight tolerances of optical

surfaces (i.e. Sa < 10 nm, PV < 100 nm), this cannot be achieved without additional means to adjust the cutting edge position to an identical fly-cut radius. In order to understand the required tolerances and importance of tool setting for milling of optical surfaces, one has to take a look at the geometric conditions during cutting (Figure 1).

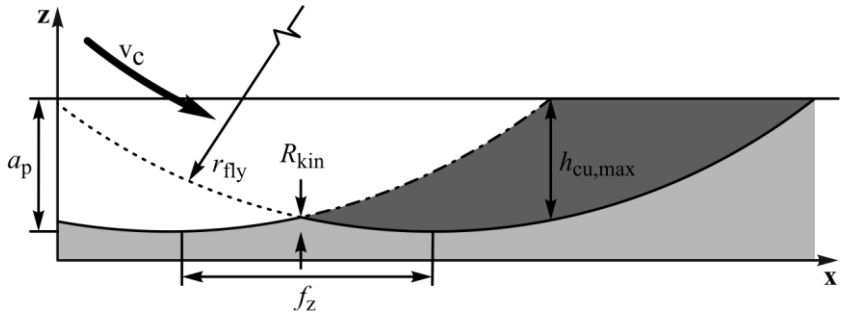

Figure 1: Cutting conditions of milling operations.

Optical surfaces are typically classified as having a surface roughness below 10 nanometres. For milling operations, the resulting kinematic roughness R_{kin} in cutting direction can be easily derived from the fly-cut radius r_{fly} and the applied feed per tooth f_z (Eq. 1).

$$R_{kin} = f_z^2 / 8 \cdot r_{fly} \qquad \text{Eq. 1}$$

For all cutting edges to contribute to the generation of the surface topography, the difference in the fly-cut radius Δr_{fly} has to be smaller than the desired kinematic roughness (Eq. 2).

$$\Delta r_{fly} \overset{!}{\leq} R_{kin} \qquad \text{Eq. 2}$$

In case that the difference in fly-cut radius is larger, the subsequent cutting edges may still contribute to the actual material removal, if Δr_{fly} is below the maximum thickness of the uncut chip $h_{cu,max}$ (Eq. 3).

$$h_{cu,max} = f_z \cdot (2\, a_p / r_{fly})^{1/2} \qquad \text{Eq. 3}$$

With a_p being the given depth of cut (typically $a_p \approx 20$ µm).

These calculations imply that the use of multiple cutting edges in a diamond milling operation requires a possibility to adjust the individual fly-cut radius with a precision of < 10 nm within the tolerances that result from the assembly of the tool holder, including the position of the cutting edges (here, a range of 500 µm is considered to be sufficient).

Several attempts have been made to introduce adjustable tool holders to diamond milling. However, mechanical solutions hardly achieve the required precision. Furthermore, the resulting centrifugal forces and thermal influences during cutting induce further deviations of the cutting edge position and thus make a pre-process setting obsolete. As a consequence, an in-process control of the cutting edge position is mandatory. The problem here is that introducing additional actuators to the fly-cutter, i.e. piezoelectric stacks, requires the

integration of additional electronics to a rotating system, to ensure power supply of the actuators and return a feedback from the position sensors.

2 Design of a thermal actuator

A novel concept for a high precision actuating mechanism is the design of a thermal actuator for positioning the individual cutting edges. The idea is to heat up the metal substrate of the tool holder locally in order to induce a controlled thermal expansion. The advantage of such a system is the fact that thermal energy can be transferred to the tool holder without the need for physical contact to the substrate, i.e. via thermal radiation (e.g. laser pulses, cf. Figure 2) or electromagnetic induction. Another benefit is the naturally slow response time of thermal processes. This means that once a constant thermal state and thus a specific expansion ΔL_1 is reached, only minimal amounts of additional energy over long periods of time are required to keep the cutting edge at a stable position ($t_3 \ll t_2$, cf. Figure 2).

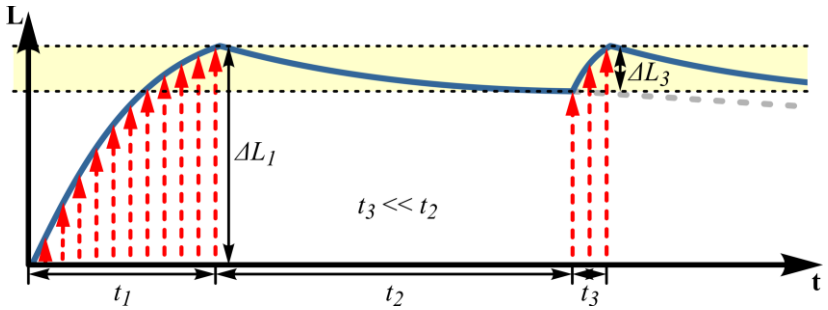

Figure 2: Controlled expansion induced by pulsed thermal radiation. t_1: time to heat to a specific expansion, t_2: contraction of substrate after interruption of energy input, t_3: short time heating to keep expansion within desired range ΔL_3.

2.1 General concept and basic calculations

The actuating mechanism was approximated as a simple 10×10×30 mm³ rectangular beam, in order to assess the required temperature differences and energy amounts for achieving the desired precision as well as the resulting maximal stroke. According to physics, the thermal expansion ΔL of such a beam can be calculated via Eq. 4, using the coefficient of thermal expansion α, the base length of the beam L_0 and the temperature difference ΔT.

$$\Delta L = \alpha \cdot L_0 \cdot \Delta T \qquad \text{Eq. 4}$$

Taking steel 42CrMo4 (α = 11.1·10^{-6} K^{-1}) as substrate material and a base length of the beam of L_0 = 30 mm, a temperature difference of $\Delta T_{\min} \approx 0.03$ K is required in order to induce a thermal expansion of ΔL_{min} = 10 nm. The maximal thermal expansion within the desired temperature range (ΔT_{max} = +10 K) is calculated to ΔL_{max} = 3.33 µm accordingly.

The amount of heat Q required to induce such a small temperature change directly affects the type and dissipated power P of the heat source that is applied. Thus, the required heat is calculated according to the mass ($V \times \rho$, with $\rho = 7850\ \mathrm{kg\ m^{-3}}$ for the applied steel) and specific thermal capacity ($c_p = 461\ \mathrm{J\ kg^{-1}\ K^{-1}}$) of the substrate using Eq. 5.

$$Q = c_p \cdot V \cdot \rho \cdot \Delta T \qquad \text{Eq. 5}$$

The following Table 1 comprises the calculated values for the required heat Q as well as for the necessary time t_{heat} to induce this heat using a given thermal power of the heat source of $P_{source} = 0.5$ W (e.g. a high-power LED). The last line shows the approximations used for the FEM simulations of chapter 2.4, that include a IR-LED source and consider a thermal absorption of 40%.

Table 1: Calculated temperature difference and amount of heat and time for inducing a controlled thermal expansion of a steel based beam shaped actuator.

Steel 42CrMo4 $\alpha = 11.1 \cdot 10^{-6}\ \mathrm{K^{-1}}$, $\rho = 7850\ \mathrm{kg\ m^{-3}}$, $c_p = 461\ \mathrm{J\ kg^{-1}\ K^{-1}}$, $V = 10 \times 10 \times 30\ \mathrm{mm^3}$				
ΔL	***ΔT***	***Q***	$\boldsymbol{t_{heat}}$	$\boldsymbol{P_{source}}$
10 nm	0.03 K	0.33 J	0.66 s	0.5 W
3.33 µm	10 K	108.85 J	217.7 s	0.5 W
5.28 nm	*0.016 K*	*0.172 J*	*1 s*	*0.43 W · 0.4*

These calculations show that a controlled thermal expansion of a beam shaped actuator can be achieved even with a low power light source in a reasonable amount of time. However, the maximal allowed temperature difference limits the resulting stroke to a value which still requires a mechanical pre-setting mechanism in order to compensate typical deviations of the setup. Therefore, the tool holder was designed to allow a pre-process mechanical tool setting for coarse adjustments and an in-process fine adjustment using a thermal actuating mechanism (Figure 3).

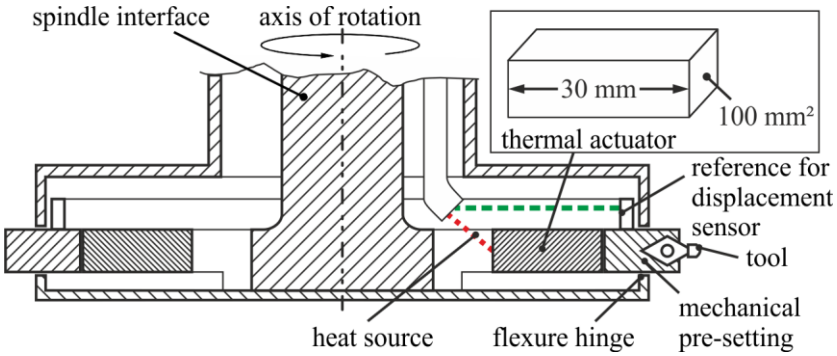

Figure 3: General concept of tool holder with thermal actuator and mechanical pre-setting mechanism.

As a general design concept, it was chosen to place the mechanical pre-setting mechanism on the outside diameter of the tool holder. This implies that this

component is also shifted, when the thermal actuator is elongated. The advantage of this arrangement is that the target area for introducing the heat remains at a constant radial position and the heat source does not need to be re-aligned after the pre-setting procedure. Furthermore, most of the heat is generated as far away as possible from where the actual cutting takes place.

2.2 Mechanism for mechanical pre-setting

The mechanical pre-setting was designed as a mechanism in which two wedges are shifted in relation to each other. When moving one of these wedges, the second one (i.e. the slide containing the tool insert) is moved with a reduced transmission ratio, due to the angle α between the two wedges. This design allows for finer adjustments than those that would be possible from the thread of the adjustment screw. Furthermore, the acting forces during cutting are absorbed in a favourable way in this configuration. The complete design of the actuator is depicted in Figure 4.

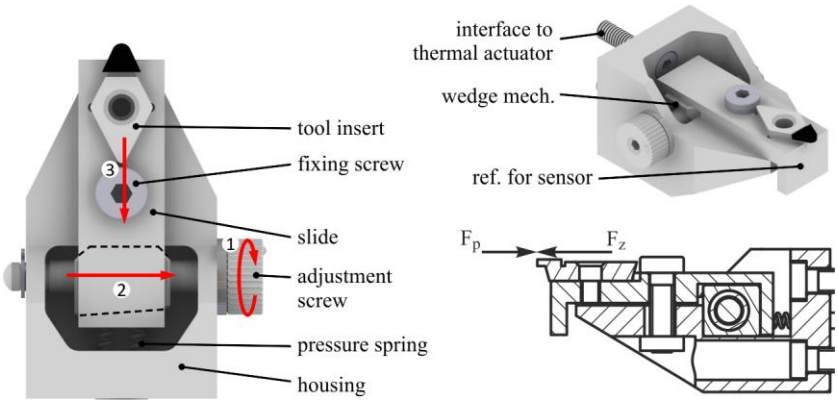

Figure 4: Mechanism for mechanical pre-setting: A fine threaded adjustment screw (1) moves a wedge mechanism (2) in order to retract the slide (3) containing the tool insert.

Due to the assumption that the acting centrifugal force at typical rotation speeds (Eq. 6) is somewhat larger than the passive force of the milling process ($F_p < 1$ N), the wedge mechanism was designed in a way that the centrifugal force acts on the wedges, while the passive force primarily acts on the screw used for clamping the slide.

$$F_r = m \cdot v^2 \cdot r^{-1} = m \cdot (2 \cdot \pi \cdot r \cdot n)^2 \cdot r^{-1} \qquad \text{Eq. 6}$$

Considering a mass of the slide of m = 0.006 kg and a radial position of the slide of r = 0.07 m, the calculated centrifugal is $F_r > 1$ N for $n \geq 466$ min^{-1}.
The adjustment screw features a thread of $P = 0.254$ mm and thus allows the first wedge to be moved approx. $S_{1min} = 15.9$ µm, considering that the screw can be rotated by hand about a minimum of 1/16th of a full revolution. With the chosen wedge angle of $\alpha = 5°$, the slide containing the tool insert can be moved

across a total distance of $S_{2max} \approx 5.25$ mm (for $S_{1max} \approx 6$ mm) with a precision of approx. $S_{2min} = 1.4$ µm (Eq. 7).

$$S_2 = S_1 \cdot \tan(\alpha) \qquad \text{Eq. 7}$$

2.3 Design of the thermal actuator

For designing the thermal actuator, a beam-shaped part was cut out of a 7.5 mm thick steel substrate (Figure 5). The actuating part is connected to the tool holder via two struts at the back. At this side, a rectangular 10 × 7.5 mm² face is provided for absorbing the thermal energy induced by the heat source. At the front of the actuator, a flexure hinge is used to provide additional stiffness against the lateral forces resulting from a cutting process (F_c and F_f). Furthermore, this end features the interface to the pre-setting mechanism.

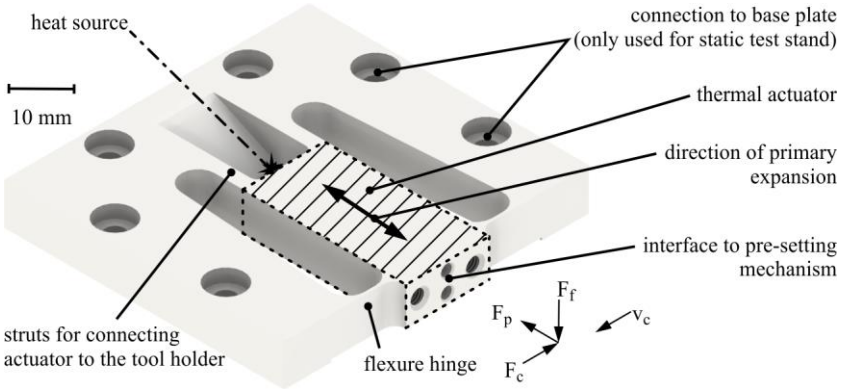

Figure 5: Design of thermal actuator.

2.4 Simulation of thermal behaviour

In order to verify the basic calculations given in 2.1, the final design of the thermal actuator was included in FEM simulations using Autodesk Simulation Mechanical 2014. This software allows the simulation of the transient heat transfer as well as the static stress that occurs while heating the part. After modelling and meshing the thermal actuator, the material properties were added and the analysis parameters were set. For obtaining a more realistic result, a thermal convection to room temperature (20 °C) was added as a constraint for all outside faces of the actuator.

The heat source was modelled directly at the target face by defining a thermal load at each node of the face. In the example presented here, a LED light source emitting at a wavelength of λ = 850 nm was modelled. It was defined that the LED illuminates a circular part of the target face covering almost its whole area. For obtaining the thermal load of each node P_{node} (Eq. 8), the total radiant flux of the LED (Φ_e = 430 mW) was divided by the amount of illuminated nodes

(n_{node} = 254) and multiplied by the coefficient of absorption for steel at this wavelength ($\eta \approx 40$ %).

$$P_{knot} = \Phi_e \cdot n_{knot} \cdot \eta = 0.677 \text{ mW/node} \quad \text{Eq. 8}$$

The total time of the simulation was set to fifteen seconds, of which the heat source was turned on for the first second and set to zero for the remaining fourteen seconds. The resulting transient heat transfer is depicted in Figure 6.

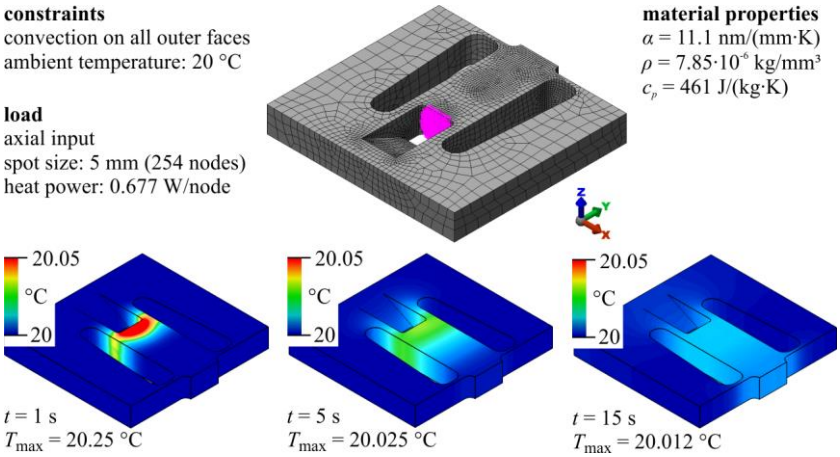

Figure 6: FEM-Simulation of transient heat transfer for thermal actuator: mesh, constraints and loads (top) and heat state at t = 1 s, 5 s and 15 s (bottom).

The simulations show that the temperature quickly rises to T_{max} = 20.25 °C after one second and then distributes along the thermal actuator in axial direction. After ten to fifteen seconds, a constant temperature level of approximately T = 20.015 °C is reached across the whole actuator. It is also shown, that the heat primarily stays within the target volume of the actuator and only small heat quantities distribute to the peripheral parts.

The results of the transient heat transfer simulations were then taken as constraints for a simulation of the thermal expansion (Figure 7).

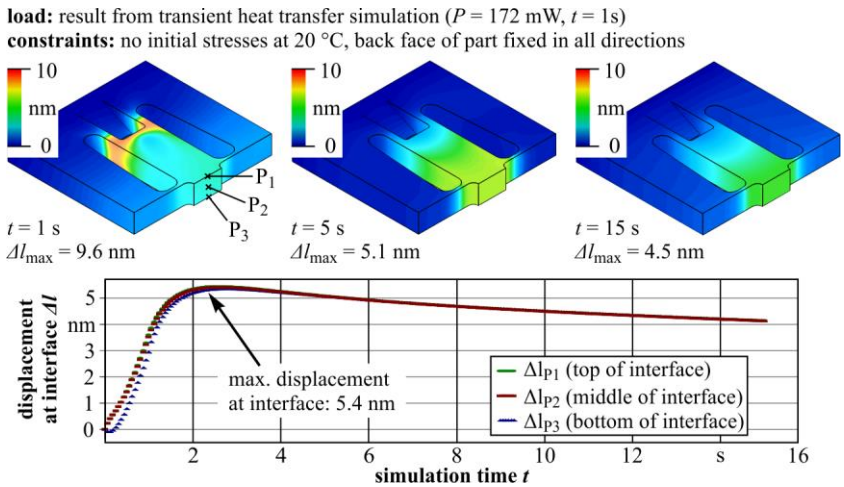

Figure 7: FEM-Simulation of thermally induced expansion: local deformation at t = 1 s, 5 s and 15 s (top images) and time-dependent axial shift of three discrete points at the tool interface (bottom graph).

The resulting displacement is measured at three discrete points on the interface to the mechanical pre-setting mechanism. Here, a maximum displacement of $\Delta l_{max} \approx 5.4$ nm was calculated. Even though the simulations considered thermal convection, this value is a bit higher than the calculations shown in chapter 2.1. A reason for this is seen in the approximation of the coefficient of absorption, which probably was chosen too small.

Nevertheless, these results show that the assumptions made for this actuator (i.e. the slow response time) are actually realistic, as the retraction of the actuator takes place gradually over several seconds.

3 Evaluation of actuating mechanism

Due to the promising results of the simulations, the designed actuator was built and installed on a static test stand (Figure 8). The displacement at the target reference plane was measured using a high-precision capacitive sensor (CPL490 with 2G-C8-1.2 picometer probe) from IBS Precision Engineering, Netherlands. This sensor is able to measure over a range of 100 µm and features a RMS resolution of 1.7 nm at a measuring frequency of 50 kHz and 0.33 nm for static measurements.

The heat source was implemented as a high-power IR-LED (OSRAM SFH 4783 "Dragon Dome"). Radiating at a wavelength of $\lambda = 850$ nm, this LED emits a total radiant flux of $\Phi_e = 430$ mW across a narrow half-angle of $\varphi = \pm 12°$, as it was modelled for the FEM simulations in chapter 2.4.

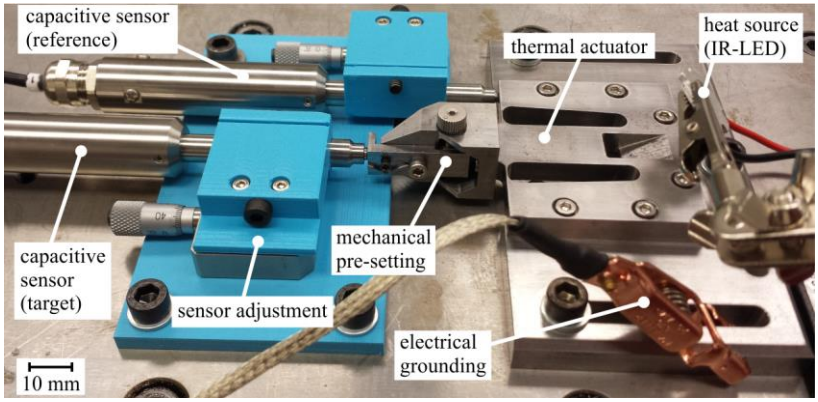

Figure 8: Static test stand for evaluating the mechanical pre-setting mechanism and the thermal actuator.

3.1 Mechanical pre-setting

For testing the repeatability of the mechanical pre-setting mechanism, the slide was moved to a defined position, which was taken as a reference. After that, the position of the slide was changed to a random position and then it was tried to reset it to the reference position. This procedure was repeated several times, in order to assess the repeatability and its uncertainty. Such a measurement cycle, showing 12 of a total of 30 measurements, is shown in Figure 9.

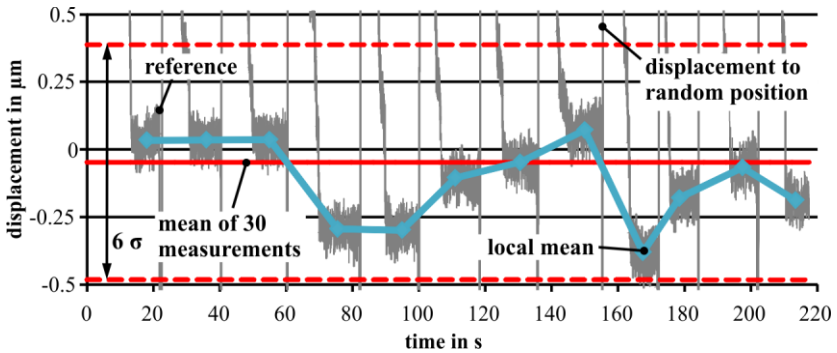

Figure 9: Evaluation of the repeatability of the mechanical pre-setting mechanism (12 of 30 measurements).

Calculating the standard deviation σ of all 30 measurements, it can be deduced that the precision ($p = 6\sigma$, i.e. 99.9 % of all measurements) of the mechanical pre-setting mechanism is $p = 0.87$ µm. This is even lower than the calculated precision for a manual 1/16 revolution of the adjustment screw and well within the requirements of the pre-setting. It means that the stroke of the thermal actuator needs to be larger than 0.87 µm in order to be able to compensate the remaining misalignment of the cutting edge.

3.2 Thermal adjustment

The thermal actuator has been evaluated by illuminating the back face with the previously described IR-LED as heat source (see Figure 8). Because measuring the thermal expansion for very short illumination times (t < 1 s) has proven to be a challenging task, the timespan for heating the thermal actuator was increased to 10 s. Nevertheless, the principal feasibility of this method can be demonstrated in this way, as shown in Figure 10.

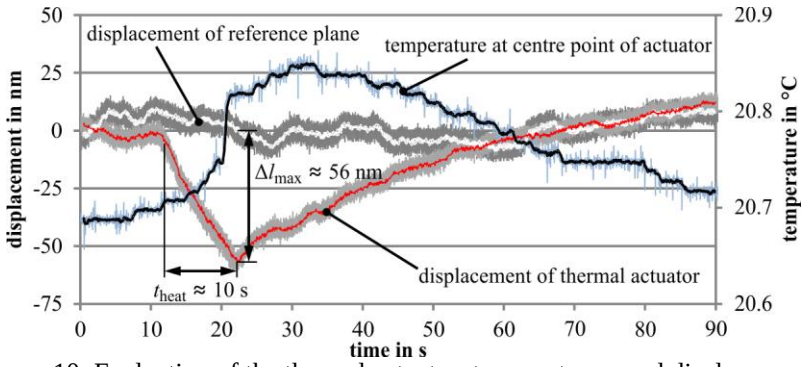

Figure 10: Evaluation of the thermal actuator: temperature ν and displacement of tool interface Δl_t and reference Δl_{ref} for heating with a Φ_e = 430 mW IR-LED for t = 10s.

Apart from the displacement at the target plane at the front of the actuator, a reference at the side of the actuator was measured, in order to rule out a general heating/expansion of the whole part. Furthermore, the temperature of the actuator was measured at its centre using a calibrated high-precision thermometer.
It can be seen, that after a couple of seconds heating time, a temperature change of ΔT = 0.15 K can be detected at the centre point of the actuator. Nevertheless, the actuator instantly starts expanding after initiating the illumination. The displacement shows an almost linear trend as long as the LED is switched on. After shutting down the heat source, the actuator instantaneously starts to retract, at a significantly slower pace. In total, a displacement of $\Delta l_{max} \approx 56$ nm was measured after t = 10s.

4 Conclusion and future work

In this paper, the design and evaluation of a thermal actuator for high-precision alignment of cutting edges in diamond milling operations was presented. According to basic calculations and FEM simulation, the performance of the actuator was assessed during the design phase. The resulting tool holder features a mechanical pre-setting mechanism and a thermal actuating part for precision adjustment. In first experiments, the performance of these actuators was evaluated and the general feasibility was shown.

The ongoing work will focus on further evaluating the performance of the thermal actuator and implementing a control system for applying this actuator in milling operations.

Acknowledgements

The authors would like to thank the German Research Foundation (DFG) for funding this work as part of subproject 1 “Ultra-precise milling with multiple diamond tools” within the research unit FOR1845 “Ultra-precision High Performance Cutting”.

References

[1] Dornfeld D, Min S and Takeuchi Y 2006 Recent Advances in Mechanical Micromachining *CIRP Ann.-Manuf. Techn.* vol 55(2) pp 745-68
[2] Brinksmeier E and Preuss W 2012 Micro-machining *Philos. T. Roy. Soc. A* vol 270 pp 3973-92
[3] Fang FZ, Zhang XD, Weckenmann A, Zhang GX and Evans C 2013 Manufacturing and measurement of freeform optics *CIRP Ann.-Manuf. Techn.* vol 62(2) pp 823-46
[4] Paul E, Evans CJ, Mangamelli A, McGlauflin ML and Polvani RS 1996 Chemical aspects of tool wear in single point diamond turning *Precis. Eng.* vol 18(1) pp 4-19
[5] Brinksmeier E, Denkena B, Kuhfuß B and Riemer O 2013 Muss Ultrapräzision zeit- und kostenintensiv sein? *Mikroproduktion* vol 13(3) pp 44-52 (in German)